A CONTRIBUTION TO THE STUDY OF WAVE PROPAGATION AND WAVE BREAKING: PHYSICAL AND NUMERICAL MODELLING

J. M. P. CONDE [1], C. J. FORTES [2], E. DIDIER [3], D. R. C. B. NEVES [4] & L. A. M. ENDRES [5]

[1] *PhD, Assistant Professor, DEMI, Faculty of Science and Technology, Universidade Nova de Lisboa (FCT-UNL), Campus de Caparica, 2829-516 Monte de Caparica, Portugal. jpc@fct.unl.pt*

[2] *PhD, Senior Research Officer, National Laboratory for Civil Engineering (LNEC), Av. do Brasil, 101, 1700-066 Lisbon, Portugal. jfortes@lnec.pt*

[3] *PhD, Post-Doctoral Fellowship Holder, National Laboratory for Civil Engineering (LNEC), Av. do Brasil, 101, 1700-066 Lisbon, Portugal. edidier@lnec.pt*

[4] *MSc, Research Grant Holder, National Laboratory for Civil Engineering (LNEC), Av. do Brasil, 101, 1700-066 Lisbon, Portugal. dneves@lnec.pt*

[5] *PhD, Associate Professor, Institute of Hydraulic Research, Federal University of Rio Grande do Sul (UFRGS), Av. Bento Gonçalves, 9500, Porto Alegre, 91501-970, Brazil. endres@ufrgs.br*

Abstract

The knowledge of the wave transformation and breaking characteristics near the coastline is essential for the design of coastal structures. This paper reports the experimental and numerical results of wave shoaling and breaking over a set of different gentle slopes. Two different numerical models are compared: a multi-layered Boussinesq model (COULWAVE) and a RANS model (FLUENT®). From the numerical tests, RANS model shows a better behavior than Boussinesq model and needs less calibration parameters; however computational time is the drawback of RANS models.

1. Introduction

The wave shoaling and breaking are important phenomena of the wave transformation in the nearshore region. The wave breaking drives to various hydrodynamic phenomena, such as wave set-up/down, wave run-up, longshore currents, nearshore circulations and so on. Therefore, the prediction of wave shoaling and breaking is essential for the nearshore hydrodynamics, as well as for the design of coastal engineering projects. More accurately, the location and extension of the wave breaking section are two of the main factors for the coastal structures foundation and stability of the nearshore sediment dynamics.

Many studies aimed to analyze the initial process of the wave breaking (*e.g.*, Goda, 1970; Weggel, 1972; Tsai *et al*., 2004; Camenen and Larson, 2007). However the processes after the initial point until the end of the wave breaking are still object of a broad discussion in the scientific community (*e.g.*, Svendsen *et al*., 1978; 2003; Tsai *et al*., 2004). The traditional wave breaking indexes are usually related with the initial location of the wave breaking, leaving in

background the end section of the process, which is, as mentioned above, especially important in coastal dynamics studies and for the setup of maritime structures.

Following this reasoning, an extensive set of experimental tests is being carried out to study the wave breaking characteristics and hydrodynamics, considering different incident conditions: regular monochromatic waves; bichromatic waves; and irregular waves. Non-breaking and breaking wave conditions are considered to allow more complete comparisons between physical experiments and numerical results.

Along with the experimental studies, two numerical tests were also performed to evaluate two types of wave propagation models: a Boussinesq model, COULWAVE (Lynett and Liu, 2004); and a Reynolds-Averaged Navier-Stokes (RANS) model, FLUENT®, version 6.3.26 (Fluent, 2006). For these tests two incident wave conditions, with the same period, T=1.5s, were considered: wave height, H=0.12m, with water level in the lee part of the bar, d=0.1m, for wave breaking condition (WBC); and H=0.10m, with d=0.3m, for non-breaking wave condition (NBWC). For these conditions, the performance of the numerical models is evaluated comparing the numerical results with the experimental data. The results presented are: a) Time series for the free surface elevation; b) Significant wave height along the flume; c) Minimum, maximum and average horizontal velocity along the flume; d) Spectral and statistical analysis.

In this paper, the experimental setup and the considered incident wave conditions are presented. The numerical models are concisely described. Time, spectral and statistical analysis data are presented. The comparison and discussion of the obtained results evaluate the ability of the models to simulate the nearshore processes.

2. Experiments

The experimental tests were performed in a wave flume (Fig. 1) at the National Laboratory for Civil Engineering (LNEC) in Lisbon, Portugal. This old regular wave flume was designed with a reduction of width to improve its hydraulic behavior, by preventing unwanted transversal waves, and, at the same time, to enable an increase of the regular wave heights (due to shoaling at the 1/11 bottom slope) produced by the limited capabilities of the original wave paddle. Nowadays is equipped with a piston-type irregular wave-maker system controlled by an A/D converter and a personal computer. This wave-maker can produce regular and irregular waves. A 10m long 1/22 slope beach profile, followed by a 10m horizontal zone was constructed. This bottom was made out of concrete so there is no permeability. At the end of the flume there is a 1/20 slope concrete bottom followed by a 1/2 slope gravel beach. Porous blankets (horsehair sheets) were installed over the 1/20 slope to reduce the reflected wave energy.

Experiments were made in three main phases, corresponding to different wave conditions: a) Regular waves resulting from the combination of four wave periods (T=1.1, 1.5, 2.0 and 2.5s) and six wave heights (H=8, 10, 12, 14, 16, and 18cm); b) Bichromatic waves resulting from a combination of two of the previous regular waves considering a certain wave height, i.e. T=1.1 and 1.5s and H=6 and 8cm; c) and irregular waves (JONSWAP spectrum) with Ts=1.5s and three different wave heights (Hs=0.12, 0.14, and 0.16m), Ts=2.0s and Hs=0.12m, and Ts=2.5s and Hs=0.12m.

For the selected wave conditions two different water depths in the lee part of the bar were considered, d=0.1 and 0.3m, in order to have breaking and non-breaking conditions.

This paper only presents results of two regular waves for two distinct water levels in the lee part of the bar: T=1.5s, H=0.1m with d=0.3m, corresponding to NBWC; and T=1.5s, H=0.12m with d=0.1m, corresponding to WBC.

Measurements consisted on time series of free surface elevations, particle velocities along the flume at the middle of the water column and velocity profiles at selected locations. Only part of these measurements is presented in this paper. Ten resistive type wave gauges were used to measure the free surface elevation. One of these probes was placed at x=-10.8m in the horizontal bottom part before the 1/22 slope to check the input condition. Eight wave gauges were placed in a mobile structure. Each gauge in this structure was separated by 20cm. Using this structure the free-surface displacement was measured from x=-10m up to x=10m. The three orthogonal components of velocity were measured by an Acoustic Doppler Velocimeter (ADV) probe. There is also a wave gauge located at the same section of the ADV. ADV measurements were made with the probe at the middle of the water column, from x=-10m up to x=8m, with a 1m interval. Velocity profiles were also measured (separated by 5 cm in the vertical direction) at selected locations. The sampling frequency of all the measurements was 25Hz, this is the maximum value of the ADV system used. The duration of the experiments was 490s, this includes an initial linear growth of the wave height and a linear decrease to zero ending. The constant wave height duration was only 4 minutes and the analysis was made only during the first two minutes of these to reduce the influence of the wave's reflections and "re-reflections". The wave breaking section (from the beginning till the end of the wave breaking zone) was defined by visual observation of a video recording.

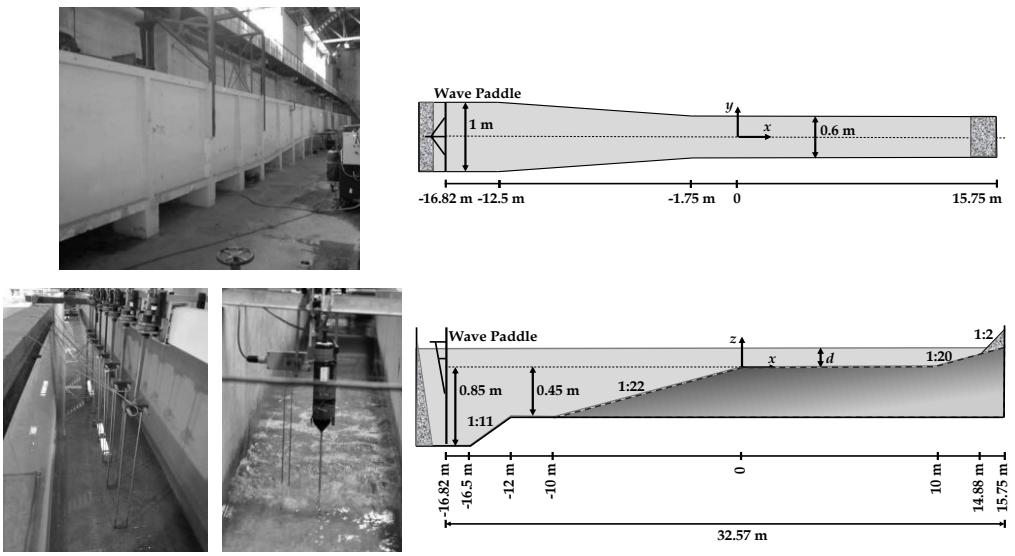

Figure 1. Wave flume (top left); wave flume's plan view (top right); 8 wave gauge mobile structure (bottom left); ADV probe and wave gauge (bottom middle); and wave flume's longitudinal-section view (bottom right).

3. Numerical models

3.1 COULWAVE code

COULWAVE (Cornell University Long and Intermediate Wave Modeling Package), a numerical model initially developed by Lynett and Liu (2004), based upon the extended Boussinesq-type equations deducted by Wei *et al.* (1995), allows modeling the evolution of fully nonlinear and dispersive waves over variable bathymetry. The model equations are deducted from the depth-integration of continuity and momentum equations, using a multi-

layer concept, which considers the division of the water column in layers, each one with a determined vertical velocity profile. The accuracy of the model is thus dependent on the number of layers considered and its applicability extends to very deep waters, as it continues to present linear characteristics up to kh~8 and a second order nonlinear behaviour up to kh~6 (where k and h are the wave number and the water depth, respectively).

Lynnet and Liu (2004) further introduced additional terms in the equations for the bottom friction, wave breaking and wave generation inside the domain and added time dependent water depth terms, in order to consider bottom-profile time variations induced by landslides and earthquakes.

To enable the Boussinesq model to simulate surf zone hydrodynamics, energy dissipation due to wave breaking is treated by introducing an eddy viscosity term into the momentum equations, with the viscosity strongly localized on the front face of the breaking waves. Wave run-up on the beach is simulated using a permeable seabed technique.

3.2 FLUENT® code

The FLUENT® code, version 6.3.26, applies a finite volume technique to solve the continuity and the RANS equations. In this code, the variables are defined in the center of each control volume. The diffusive terms of the equations are discretized by the second order central difference scheme. There are available: different interpolation schemes for the convective terms (first order Upwind, first order power law, second order Upwind, MUSCL and QUICK); different resolution algorithms (Coupled, SIMPLE, SIMPLEC and PISO); and different turbulence models (Fluent, 2006). The capture of the free surface is done by the Volume of Fluid (VoF) method. This method identifies the position of the free surface from a scalar indicator, the volume fraction, which takes the value 0 in the air and 1 in the water. The position of the free surface is arbitrarily defined by the value 0.5.

In the simulations carried out were used: the 3D module of the code; the implicit formulation; the 2nd order time discretization for NBWC and the 1st order time discretization for WBC; and the standard k-ε turbulence model. The SIMPLEC algorithm was used for both simulations. Under relaxation was used only in the equations of k and ε, the coefficients were equal to 0.8. For the convective terms in the faces of the control volumes: the components of the momentum were determined by the MUSCL 3nd order interpolation scheme; and k and ε were determined by the second order Upwind interpolation scheme. The volume fraction on the faces of the control volumes was determined by: a modified version of the High Resolution Interface Capturing (HRIC) scheme with an implicit time scheme for NBWC; and by the CICSAM scheme with an explicit time scheme for WBC. The pressure is determined by the PRESTO! (PREssure STaggering Option) scheme (Fluent, 2006).

3.3 Numerical conditions and computational domain

For the RANS model (FLUENT® code) the computational domain is equal to the physical flume, with the same bottom profile and width reduction from the wave paddle up to x=-1.75m. At the end of the numerical flume (x=10m) a numerical adsorption beach was applied to eliminate wave reflection. The numerical wave generator is located at same location as the physical wave paddle, x=-16.82m. The waves are generated by the imposition of the free surface position and the velocity components deduced from the linear wave theory. The discretization mesh, hexahedral elements, is non-uniform: being more refined in the wave propagation direction as the depth diminishes; and in the vertical direction, more refined close to the free surface and near the bottom. The mesh refinement at the free-surface zone is comprised of: 50 to 60 elements per wave length of the incident wave; and 20 elements per

wave height. The total number of control volumes is about 875000, only half of the domain was simulated, a symmetry plane condition was imposed in the wave propagation direction. The time step is equal to 0.0015s ($T/1000$), 6 nonlinear iterations at each time step were imposed. The total simulation time was 35s (23.3T).

For the Boussinesq model (COULWAVE code) the computational domain is 37.2m long, with a constant width of 1m. The code generates a finite difference grid mesh with an element size in the x direction of 0.05m. The Courant number imposed is equal to 0.2. The waves are generated by a source function located at x=-16.82m. Two boundary absorption layers are located at each end of the domain. The bottom friction is not considered. The total time of simulation was 300 s (200T).

The Boussinesq model simulations were performed in a personal computer (PC) with a 2.80GHz Intel® Core™ i5 processor and 3.46GB of RAM. The RANS model simulations were performed in a PC with a 2.67GHz Intel® Core™ i7 920 processor and 8.0GB of RAM. The simulation time for the Boussinesq model was 6 minutes for 300s of flow simulation, and about 5 and ½ hours per wave period for the RANS model.

4. Results and discussion

4.1 Wave height

Comparison between numerical results and data measured in the physical tests is made for the wave heights and velocities. Figures 2 and 3 display the wave height comparison between the measurements and numerical models results along the flume, for NBWC and WBC.

The experimental wave height increases along the flume, due to shoaling and flume's width reduction, up to: x=2m, for NBWC (Fig. 2); and x=-3m, for WBC (Fig. 3). This behavior is followed by the RANS model simulations, with a little attenuation. The Boussinesq model is unable to reproduce the wave height increase; this may be due to model limitations and also due to the constant flume width simulation. After wave breaking both models tend to reproduce relatively well the experimental data (Fig. 3).

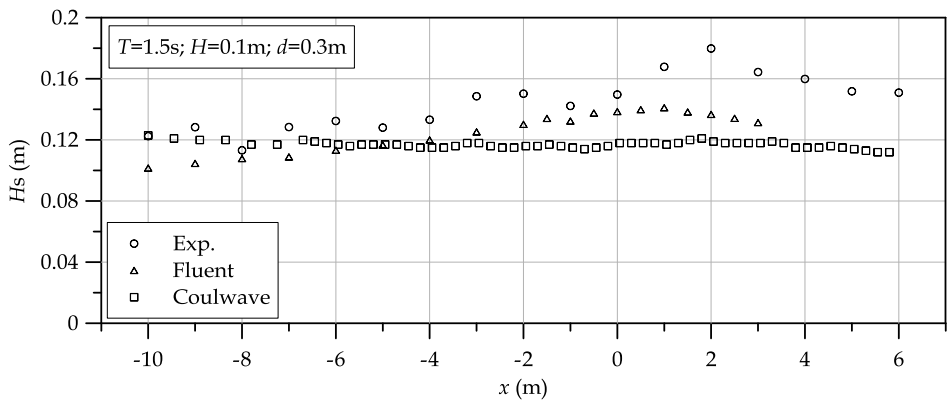

Figure 2. Experimental and numerical significant wave height, Hs, along the flume for non-breaking wave condition (NBWC).

The disagreement between the numerical and experimental values may also be related to the input data on the wave maker. Notice that, in both models, the input conditions at the paddle location are: significant wave height, for the Boussinesq model; and surface elevation and velocities (vertical and horizontal, calculated from linear theory) for the RANS model.

These are not the same that occur on the experimental flume. In fact, the vertical profile of the input velocities was not measured near the wave maker location, so the input velocities could not be compared and the differences could have an influence on the results.

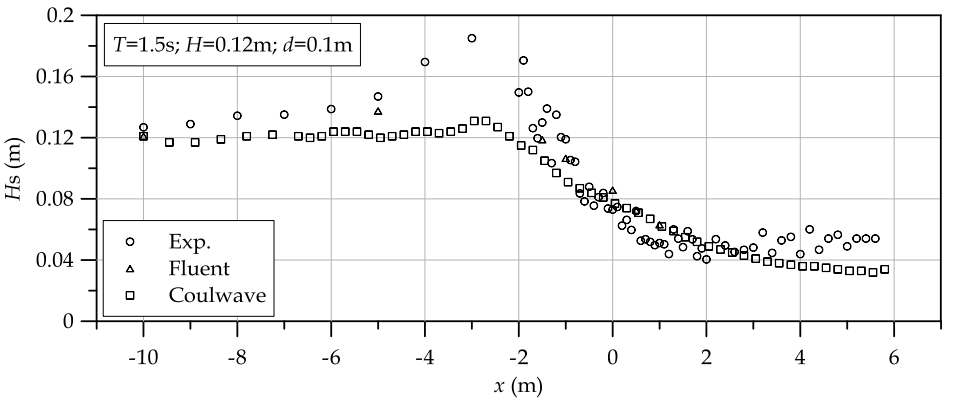

Figure 3. Experimental and numerical significant wave height, *Hs*, along the flume, for the wave breaking condition (WBC).

4.2 Free surface elevation and spectra

Figure 4 displays the comparison of the free surface elevation time series (figures on the left side), and the corresponding spectra (figures on the right side), between the measurements and the numerical results, at x=-10, -6, -2, and 0m, for a NBWC incident regular wave, with T=1.5s and H=10cm.

From the free surface elevation figures is clearly visible the wave transformation, due to shoaling, as the wave propagates along the channel. The spectral analysis shows the increasingly number of harmonics and the strong reduction on the amplitude of the main frequency. The numerical results present a similar behavior to the experimental, but with lower amplitude, as previously viewed in figure 2. As in figure 2, the Boussinesq model presents lower values than the RANS model.

4.3 Velocity

Figures 5 and 6 present the experimental data and the numerical results of the average longitudinal velocity, V_x, and the average envelope (maximums and minimums) of longitudinal velocity, for non-breaking and breaking wave conditions.

The average of the velocity values at each record was calculated through the average of all measured values in the record. The averages of the maximum and minimum velocities were calculated by the identification of each "individual wave" using the downward zero crossing criterion. Each intersection was considered effective when there were at least two points before and after the zero reference.

For the NBWC (Fig. 5) the average experimental value is constant and equal to zero in the entire flume. The minimum and maximum values present symmetry up to around x=-4m. After this position and up to the end of the flume, the maximums are higher than the minimums, which is consistent with the asymmetric free surface elevation presented in Fig. 4. Boussinesq model reproduces the experimental values with some attenuation which is consistent with Fig. 2 results.

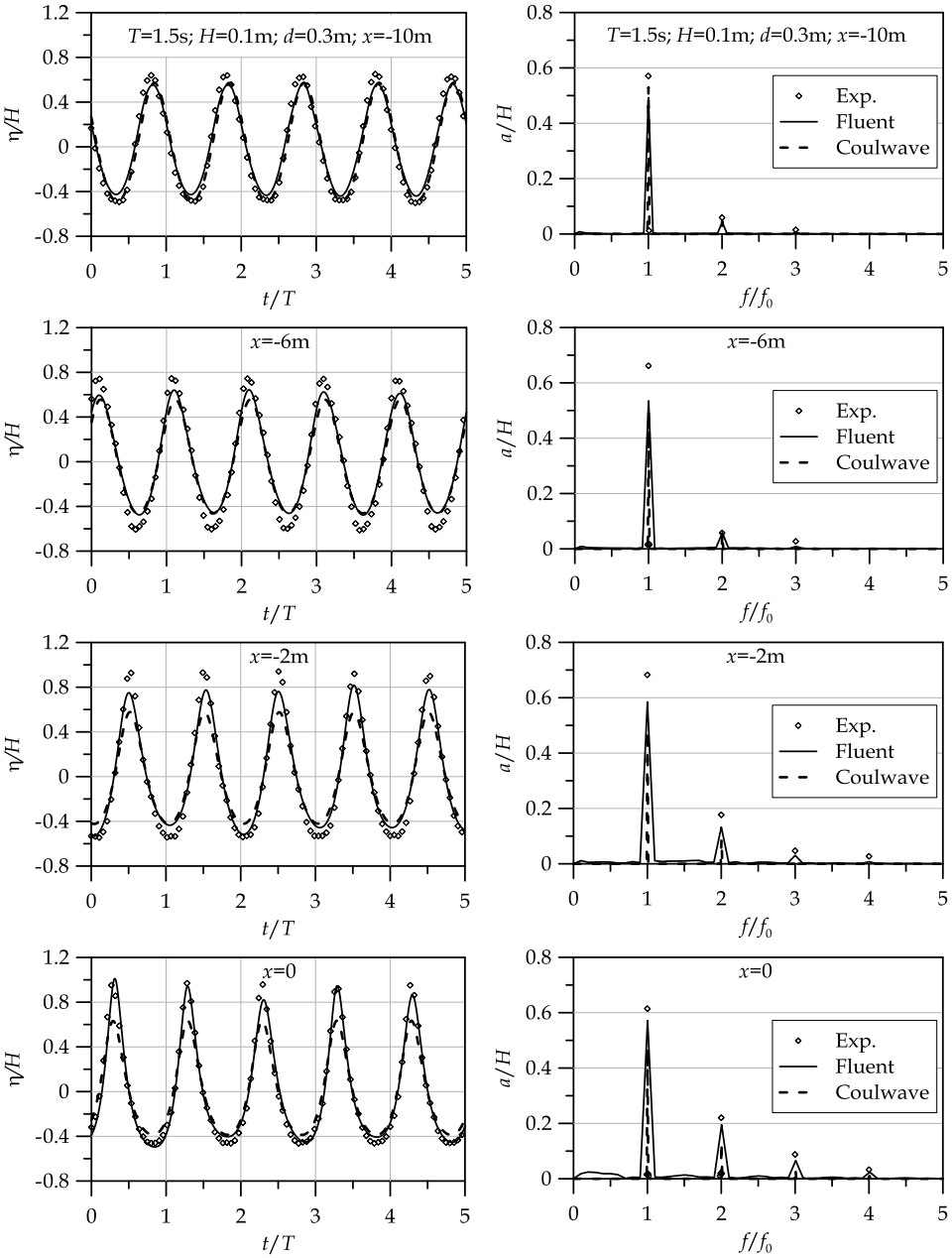

Figure 4. Experimental and numerical free-surface elevation, η, and amplitude spectrum, a, at different locations along the flume, for NBWC.

As observed in figure 6, after the breaking point (near x=-2m), the average values of V_x velocities start to decrease till become almost constant by the end of the wave breaking (near x=2.5 m). Also, there is a small return flow (negative V_x values) before the initiation of the wave breaking, however this small flow proves to be very small comparing with the wave

breaking section values, the Stokes drift can explain the values presented, they reflect the typical onshore flow in such conditions. After the wave breaking, due to the horizontal bottom, the values are proved to be very close to zero.

The numerical values presented in figure 6 are consistent with the ones presented in figure 4 for NBWC. RANS model results reproduce the experimental values with some attenuation, while Boussinesq model results are quite apart from the experimental data showing a smooth variation in the wave breaking zone.

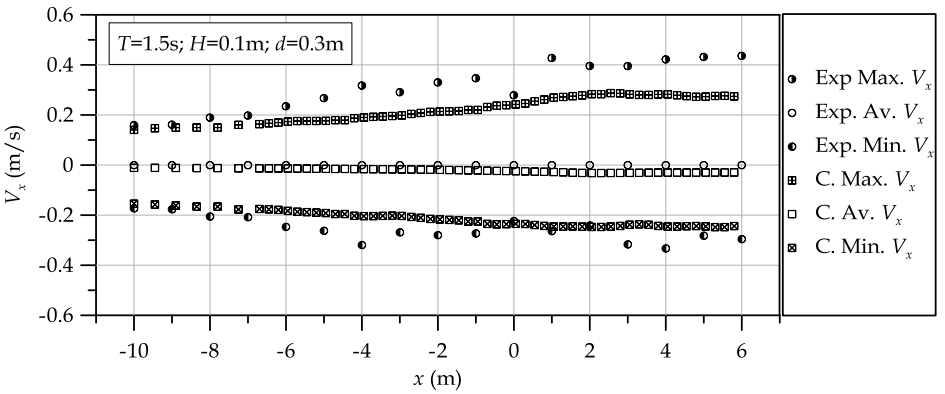

Figure 5. Experimental and numerical average longitudinal velocity, V_x, and average envelope (maximums and minimums) of the longitudinal velocity, for NBWC. (C. – Coulwave)

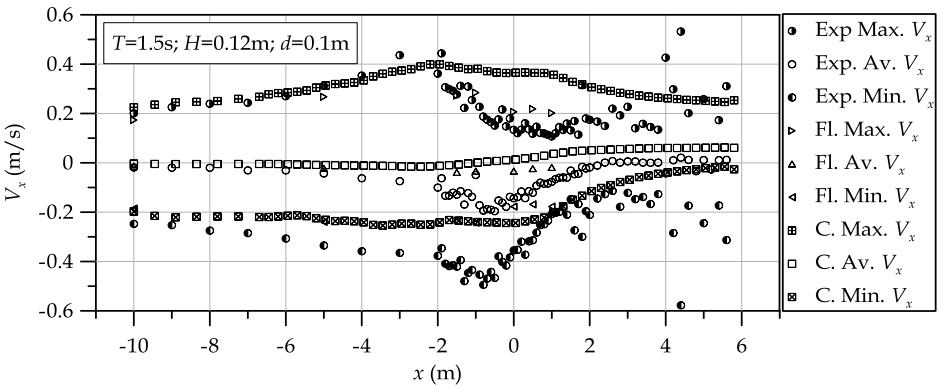

Figure 6. Experimental and numerical average longitudinal velocity, V_x, and average envelope (maximums and minimums) of the longitudinal velocity, for WBC. (Fl. – Fluent, C. – Coulwave)

4.4 Statistical analysis

Tables 1 and 2 present the statistical analysis, the quantities are the bias, the root mean square error (r.m.s.e.) and the concordance index (c.i.), defined by Eq. [1], for NBWC and WBC, respectively.

$$\text{bias} = \frac{\sum_{i=1}^{n}(y_i - x_i)}{n}; \qquad \text{r.m.s.e.} = \sqrt{\frac{\sum_{i=1}^{n}(y_i - x_i)^2}{n}}; \qquad \text{c.i.} = 1 - \frac{\sum_{i=1}^{n}|y_i - x_i|^2}{\sum_{i=1}^{n}\left(|y_i - \overline{x}| + |x_i - \overline{x}|\right)^2} \quad [1]$$

where x_i and y_i are the experimental and the numerical values, respectively.

The H_s values presented in Tables 1 and 2 show that, with an r.m.s.e. higher that the RANS model results, Boussinesq model results are lower than the experimental data (negative bias). For NBWC, the c.i. for the Boussinesq model (97.4%) is lower than the RANS model value (98.5%), as expected. For WBC, the c.i. values are equal for both models (99.9%).

Table 2 shows that the WBC V_x bias and r.m.s.e. values are positive (numerical values higher that the experimental data) for both Boussinesq and RANS models. The average values of V_x are lower for the Boussinesq model, while the maximums and minimums values are lower for the RANS model. The c.i. for the V_x values is lower than the c.i. for the H_s values for both models.

Table 1. Statistical analysis for non-breaking wave condition.

	H_s		
MODEL	**bias (cm)**	**r.m.s.e (cm)**	**c.i.**
FLUENT	-2.073	2.181	0.985
COULWAVE	-2.540	2.945	0.974

Table 2. Statistical analysis for wave-breaking condition.

	H_s			AVERAGE OF MINIMUMS OF VELOCITY			AVERAGE VELOCITY			AVERAGE OF MAXIMUMS OF VELOCITY		
MODEL	**bias (cm)**	**r.m.s.e (cm)**	**c.i.**	**bias (cm)**	**r.m.s.e (cm)**	**c.i.**	**bias (cm)**	**r.m.s.e (cm)**	**c.i.**	**bias (cm)**	**r.m.s.e (cm)**	**c.i.**
FLUENT	-0.015	0.963	0.999	11.58	12.94	0.92	6.40	7.52	0.96	3.20	6.73	0.98
COULWAVE	-0.734	1.592	0.999	9.07	10.62	0.94	9.79	11.16	0.94	14.39	17.77	0.95

5. Conclusions

In this paper, physical modeling tests on a wave flume at the National Laboratory of Civil Engineering (LNEC) in Lisbon were presented. The tests aimed to study the wave propagation and the wave breaking hydrodynamics on a beach profile with different bottom slopes since its beginning till the very end. From these tests a wide set of wave data (free surface elevation and particle velocity) along the flume and especially in the wave breaking section is available. This constitutes an important output of this work since it can be used to understand more deeply the wave propagation process but also for the establishment/improvement of the wave breaking numerical models and its validation.

The models simulate the wave propagation characteristics along this 3D Flume with some limitations. The RANS model has a better behavior than the Boussinesq model, as expected, for both cases and especially for wave breaking conditions. The models limitations may be due to several reasons:

- The wave generation method of the numerical models are different from the piston-type experimental wave-maker: for the Boussinesq model the free surface elevation is imposed as a boundary condition; for the RANS model the free surface elevation and the velocity profile (vertical and horizontal components) are imposed at the wave-maker location;
- The Boussinesq model is a depth-integrated model, which in the surf zone has its limitations;
- The Boussinesq model does not reproduce the variation of the flume width;
- Usually, for the RANS model, the mesh discretization should correspond to 60 threads per wavelength. This criterion is met for the fundamental frequency, which is not the case for the harmonics (35 segments for the first harmonic). The harmonics are thus dispersed.

From the numerical tests, RANS model shows a better behavior then Boussinesq model and needs less calibration parameters; however computational time is the drawback for the RANS models.

As future work, other numerical models may be tested for these experimental test cases to improve the quality of the results. These models may be different from the ones tested here, or could be improved versions or approaches on these models, *e.g.*, different turbulent models for the RANS model.

Acknowledgments

This work has been developed at LNEC within the scope of the J. M. P. Conde sabbatical leave from Universidade Nova de Lisboa (Portugal) and L. A. M. Endres sabbatical leave from Federal University of Rio Grande do Sul (Brazil). The support by the FCT projects HIDRALERTA and EROS and FCT/CAPES project ''Building a research and knowledge basis for Coastal Engineering '' (cooperation Portugal/Brazil) are also acknowledged.

References

Camenen B., Larson M. 2007. 'Predictive Formulas for Breaker Depth Index and Breaker Type', *Journal of Coastal Research,* volume 23, issue 4, 1028 – 1041.

Fluent Inc. 2006. 'FLUENT 6.3 User's Guide', Fluent Inc., Lebanon, NH.

Goda Y. 1970. 'A Synthesis of Breaking Indices', *Transactions of JSCE*, volume 2, part 2, 39-49.

Lynett P., Liu P.L.F. 2004. 'Modelling wave generation, evolution and interaction with Depth -Integrated, Dispersive Wave equations'. COULWAVE Code Manual. Cornell Univ. Long Inter. Wave Modelling Package.

Svendsen I.A., Madsen P.A., Hansen J.B. 1978. 'Wave characteristics in the surf zone', *Proc. of 16th ICCE*, 520-539.

Svendsen I.A., Qin W., Ebersole B.A. 2003. 'Modelling waves and currents at the LSTF and other laboratory facilities', *Coastal Engineering*, 50, issues 1-2, 19-45.

Tsai C.P., Chenb H.B., Hwungc H.H., Huang M.J. 2004. 'Examination of empirical formulas for wave shoaling and breaking on steep slopes', *Ocean Engineering*, volume 32, issues 3-4, 469-483.

Wei, G., Kirby, J.T. (1995). Time-dependent numerical code for extended Boussinesq equations. J. Waterways, Ports, Coastal and Ocean Eng., ASCE, pp. 251-261.

Weggel, J.R. 1972. 'Maximum Breaker Height', *Journal of Waterways, Harbors, and Coastal Engineering Division*, volume 98, 529-554.